Fabrication of silica pyramids by enhanced lateral etching of hydrofluoric acid below metal films

R. Kirchner, V. Neumann, F. Winkler, C. Strobel, S. Völkel, A. Richter, J. W. Bartha
TU Dresden, Institute of Semiconductors and Microsystems, 01062 Dresden, Germany
robert.kirchner@tu-dresden.de

D. Kazazis
Paul Scherrer Institute, Laboratory for Micro- and Nanotechnology, 5232 Villigen PSI, Switzerland

The fabrication of inverted pyramids in crystalline silicon is based on anisotropic etching of different crystal planes.[1] Anisotropic etching of amorphous silica in hydrofluoric acid (HF) not expected.[2] Etch enhancement due to Ti and Al layers was observed for liquid and vapor phase HF on silicon dioxide.[3,4] We used, for the first time, a controlled etch behavior beneath certain metal pads to create ultra-sharp and self-perfecting silica pyramids.[5] This has impact on capillary stamping, plasmonics, photovoltaics and light emitting diodes for example.
Metal pads were obtained via mask-aligner lithography, electron beam metal evaporation and lift-off. Beneath square-shaped metal pads, square-base pyramids were obtained for different aqueous HF solutions (Fig. 1). Unbuffered (Fig. 1 a-d) and buffered (Fig. 1 e-h) etching yielded perfect pyramids due to enhanced etching along the metal-silica interface. The selectivity for the buffered etch was higher enabling shallower pyramids. For highly concentrated HF (Fig. 1 i-l) the selectivity was much smaller (Tab. 1). Different metals resulted in different lateral etch rates of the metal-silica interface. The fastest etching occurred for the 5 nm Ti adhesion layer with 50 nm Cr layer (21.5 nm s^{-1}) compared to the same Au or Pt thickness (11.4-12.8 nm s^{-1}) or 50 nm Cr without Ti layer (14.1 nm s^{-1}). Ti alone cannot fully explain this. We assume a modified interface in general. Similar structures were obtained for vapor phase etching (Fig. 3) due to condensation and capillary forces attracting liquid HF below the metal pads.
In conclusion, 3D surface relief structures in amorphous layers such as thermal silicon dioxide, fused silica or borofloat glass could be realized using a generalized process.

---

[1] H. Seidel, L. Csepregi, A. Heuberger, H. Baumgärtel, J. Electrochem. Soc. 137 (11), 1990.
[2] P. C. Simpson, A. T. Woolley, R. A. Mathies, Biomed. Microdev. 1 (1), 1998.
[3] N. Pekas, Q. Zhang, M. Nannini, D. Juncker, Lab Chip 10, 2010.
[4] R. Kometani, M. Okuno, S. Warisawa, in Proc. 62nd Int. Conf. Electron, Ion Photon Beam Techn. Nanofab. (EIPBN) (Puerto Rico, 2018), (A4-2).
[5] R. Kirchner, V. Neumann, F. Winkler, C. Strobel, S. Völkel, A. Hiess, D. Kazazis, U. Künzelmann, J. W. Bartha, Small 16 (43), 2020.

.

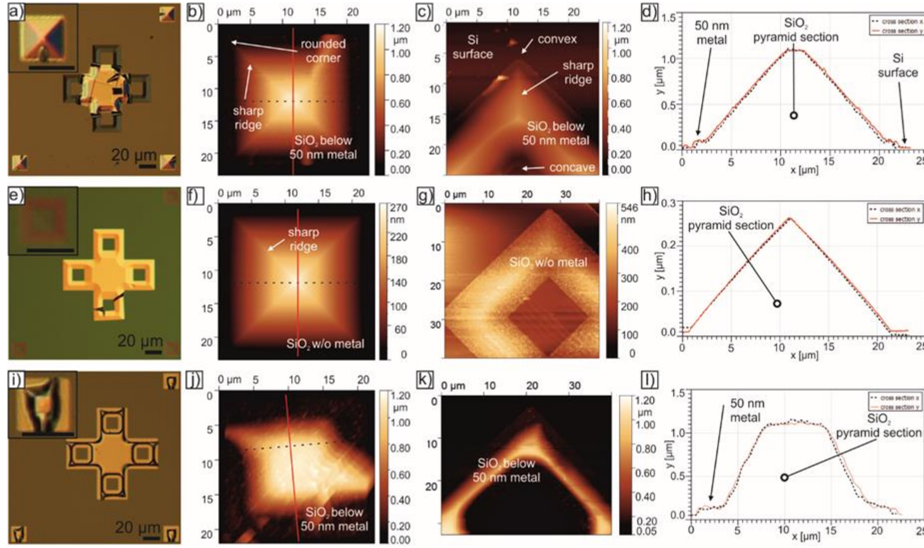

Figure 1 Topography with and without 5 nm Ti/50 nm Au overlay film after applying different wet etchants: a-d) 10 min BOE etching (w/ overlay), e-h) 10 min 5% unbuffered HF (w/o overlay), i-l) 2 min 50% unbuffered HF (w/ overlay).

Table 1 Etch behavior of different etchants used on 1 µm wet thermal SiO_2 on {100} silicon substrates with 5 nm Ti/ 50 nm Au masking. (BOE: buffered oxide etch, HF: hydrofluoric acid, IPA: isopropyl alcohol).

	BOE ≈5% HF	**5% HF unbuff.**	**50% HF unbuff.**	**4:1 50% HF:IPA vapor / 40 °C**
Vertical rate r_v (nm s^{-1})	1.8	0.4	7.5	0.14 (v)
Lateral rate r_l (nm s^{-1})	15.7	17.2	42.9	8.3 (l)
Inclination *(°)	6.5	1.3	9.7	1.0
Ratio r_l / r_v	8.7	43.0	5.7	59.3

(v): vapor phase etching, (l): liquid phase etching due to condensation)
* estimated from ratio r_l/r_v, r_l: lateral etch rate, r_v: vertical etch rate.

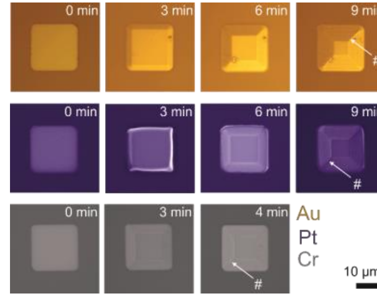

Figure 2 Under-etch behavior of different metal masks, also confirming corner sharpening and self-perfection (#).

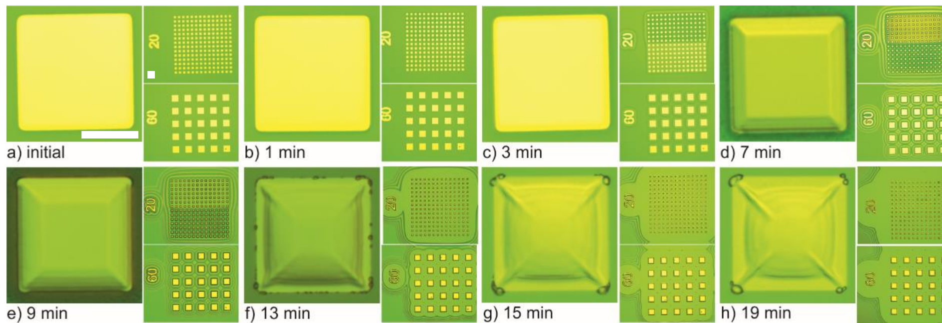

Figure 3 Vapor-phase HF etching of 5 nm Ti/50 nm Au pads: b-e) Clear pyramidal etching observed. f-h) metal-Si surface contact leading to surface deformation (wrinkling visible) (scale bar 10 µm).